

Supporting Information

Efficient photocatalytic hydrogen production by organic–inorganic heterojunction structure in $\text{Chl@Cu}_2\text{O}/\text{Ti}_3\text{C}_2\text{T}_x$

Yuanlin Li^a, Yanxiang Liu^a, Tianfang Zheng^a, Aijun Li^a, Georgiy G. Levchenko^a, Wei Han^{b,*},
Aleksy V. Pashchenko^c, Shin-ichi Sasaki^{d,e}, Hitoshi Tamiaki^d and Xiao-Feng Wang^{a,*}

^a *Key Laboratory of Physics and Technology for Advanced Batteries (Ministry of Education) & State Key Laboratory of Superhard Materials, College of Physics, Jilin University, Changchun 130012, P. R. China*

^b *College of Physics, State Key Laboratory of Inorganic Synthesis and Preparative Chemistry, International Center of Future Science, Jilin University, Changchun 130012, P. R. China*

^c *Donetsk Institute for Physics and Engineering named after O.O. Galkin, NAS of Ukraine, Kyiv 03028, Ukraine*

^d *Graduate School of Life Sciences, Ritsumeikan University, Kusatsu, Shiga 525-8577, Japan*

^e *Department of Medical Bioscience, Faculty of Bioscience, Nagahama Institute of Bio-Science and Technology, Nagahama, Shiga 526-0829, Japan*

* Corresponding authors.

E-mail addresses: whan@jlu.edu.cn (Wei Han), xf_wang@jlu.edu.cn (Xiao-Feng Wang).

Experimental section

Synthesis of Chl and $\text{Ti}_3\text{C}_2\text{T}_x$ MXene

Chl was prepared as previously reported^{S1,S2}. $\text{Ti}_3\text{C}_2\text{T}_x$ MXene was obtained by etching Ti_3AlC_2 (Forsman, 98%) in 49% HF solution at room temperature as follows. First, 10 mL of HF was added to 50 mL of plastic beakers under continuous stirring at 300 rpm for several minutes. Then 1 g of Ti_3AlC_2 MAX powder was slowly added to the etchant solution and continuously reacted for 24 h at room temperature. The obtained solution was washed and centrifuged with deionized water several times until neutral pH was reached. When the neutral solution of $\text{Ti}_3\text{C}_2\text{T}_x$ was obtained, the $\text{Ti}_3\text{C}_2\text{T}_x$ sediment was collected after discarding the supernatant. Finally, the mixture was dried in a vacuum oven at 50 °C for 12 h to obtain $\text{Ti}_3\text{C}_2\text{T}_x$ MXene nanosheets.

Preparation of Chl@ $\text{Cu}_2\text{O}/\text{Ti}_3\text{C}_2\text{T}_x$ composites

Chl@ $\text{Cu}_2\text{O}/\text{Ti}_3\text{C}_2\text{T}_x$ composites were obtained by a stepwise deposition process of Cu_2O and Chl as follows. First, 67.87 mL of deionized, 0.75 mL of CuSO_4 (0.1 mol/L) solution and 3 mg of $\text{Ti}_3\text{C}_2\text{T}_x$ were added to a beaker and were sonicated for 30 min. Then, 2.63 mL of NaOH (1 mol/L) was added dropwise to the above solution. After that, 3.75 mL of 0.2 mol/L ascorbic acid (AA) was added and the obtained solution was left to stand for 3 h. Afterwards, the obtained samples were processed by high speed centrifugation and the solid precipitates were washed twice with water-ethanol mixture ($V_{\text{water}}:V_{\text{ethanol}} = 1:1$). At the same time, the $\text{Cu}_2\text{O}/\text{Ti}_3\text{C}_2\text{T}_x$ samples were obtained by drying at 35 °C for 12 h. Next, $\text{Cu}_2\text{O}/\text{Ti}_3\text{C}_2\text{T}_x$ (3 mg) was added to a tetrahydrofuran (THF) solution of Chl. The mass ratio

of Chl to $\text{Cu}_2\text{O}/\text{Ti}_3\text{C}_2\text{T}_x$ was 1% (30 μg), 2% (60 μg), 4% (120 μg) or 8% (240 μg), respectively. The $\text{Chl}@/\text{Cu}_2\text{O}/\text{Ti}_3\text{C}_2\text{T}_x$ mixture was stirred at room temperature for 10 h until the solvent was completely evaporated. The collected dried sample is the required $\text{Chl}@/\text{Cu}_2\text{O}/\text{Ti}_3\text{C}_2\text{T}_x$ composite.

Characterization

To characterize Chl, Cu_2O , $\text{Ti}_3\text{C}_2\text{T}_x$ and the composites, an X-ray diffraction (XRD, D8 Advance, Bruker) was operated at 40 kV and 200 mA with Cu $\text{K}\alpha$ radiation ($\lambda = 0.15406$ nm). Scanning electron microscopy (SEM, SU8000, Hitachi) was used to observe the morphology of the samples. The energy-dispersive X-ray spectroscopic (EDS, Magellan400) mapping was measured to investigate the distribution of the composite elements. Fourier transform infrared spectroscopy (FT-IR, Vertex70, Bruker) was used to obtain the spectra of the samples in a range of 400 to 3100 cm^{-1} . Electronic absorption spectra of samples were measured with a UV-visible absorption spectrometer (UV-3600, Shimadzu). X-ray photoelectron spectroscopy (XPS) was performed on a Thermo Scientific NEXSA spectrometer with Al $\text{K}\alpha$ radiation excitation source. The electrochemical impedance spectroscopic (EIS) measurements in the range from 0.1 Hz to 100 kHz and the transient photocurrent (TPC) response were carried out with an electrochemical workstation (Bio-Logic SAS) in a standard three-electrode system. The steady-state photoluminescence (PL) was measured on a Shimadzu RF-6000 spectrophotometer. Specific surface area measurements (Kubo-X1000) were typically based on N_2 sorption with pretreatment at 60 °C under the Brunauer-Emmer-Teller (BET) model.

Photocatalytic activity measurements

Photocatalytic H₂ evolution was measured under a 300 W Xenon lamp (PLS-SXE 300, Beijing Perfectlight Technology): the light intensity was 100 mW/cm². A 6 mL photoreactor and a cut-off filter (usually $\lambda > 420$ nm) were used. Chl@Cu₂O/Ti₃C₂T_x photocatalysts composite (3 mg) was added in an aqueous 55 mM AA solution (3 mL). The mixture was sonicated for 5 min before light irradiation to fully disperse the composite. Argon was purged to remove oxygen in the solution and the reactor for 10 min. The reactants were continuously stirred under irradiation for 2 h. The hydrogen production was measured by a gas chromatograph (SP-3420A, Beijing Beifen-Ruili Analytical Instrument) with a thermal conductivity detector. The carrier gas was argon and the column contained 5 Å molecular sieves. The average values were obtained by five independent experiments.

The N₂ adsorption-desorption isotherm of Ti₃C₂T_x is shown in Figure S1. The specific surface area of the Ti₃C₂T_x sample obtained by BET measurements was 6 m²/g.

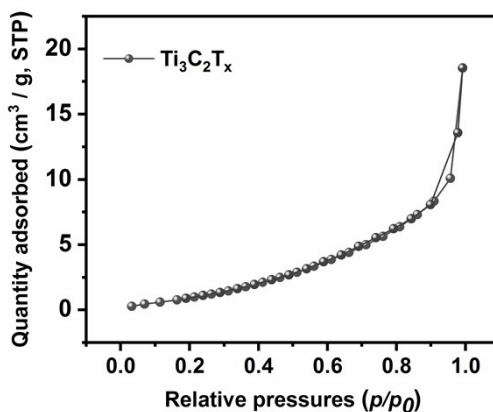


Figure S1. N₂ adsorption-desorption isotherm of Ti₃C₂T_x.

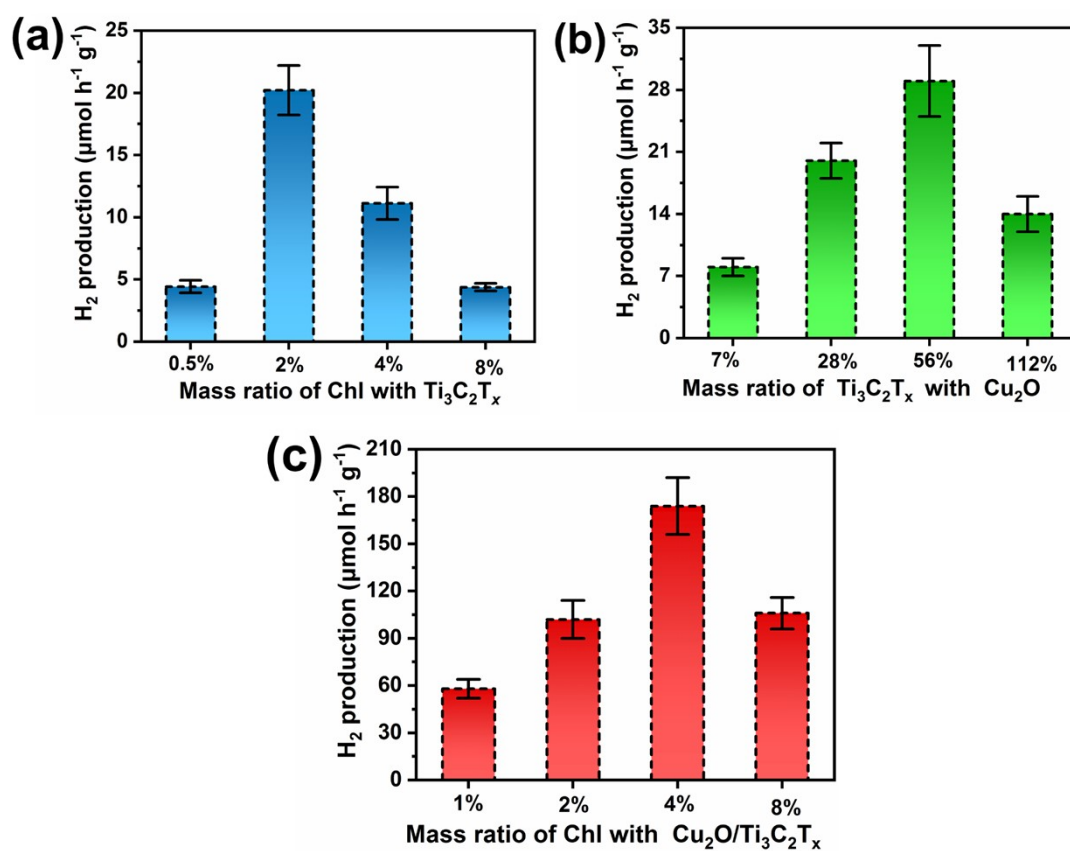


Figure S2. Hydrogen production of Chl@Ti₃C₂T_x, Cu₂O@Ti₃C₂T_x and Chl@Cu₂O/Ti₃C₂T_x composites with different mass ratios (a-c) under white light illumination ($\lambda > 420$ nm).

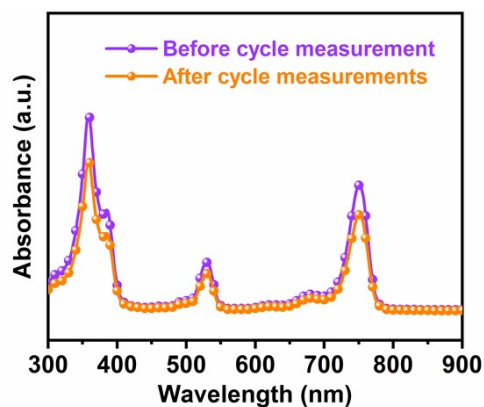


Figure S3. UV-visible absorption spectra in THF before/after Chl@Cu₂O/Ti₃C₂T_x cycle

measurement.

Figure S4 shows the reactivation measurements of the photocatalytic HER performance of the $\text{Chl@Cu}_2\text{O/Ti}_3\text{C}_2\text{T}_x$ sample. First, the $\text{Chl@Cu}_2\text{O/Ti}_3\text{C}_2\text{T}_x$ samples after three cycling measurements were recovered by high-speed centrifugation. Then, $\text{Chl@Cu}_2\text{O/Ti}_3\text{C}_2\text{T}_x$ was dried in a vacuum drying oven at 60 °C for 12 h to obtain the required samples. The $\text{Chl@Cu}_2\text{O/Ti}_3\text{C}_2\text{T}_x$ sample was obtained by redepositing 1% mass ratio of Chl. Finally, fresh AA solution was added to $\text{Chl@Cu}_2\text{O/Ti}_3\text{C}_2\text{T}_x$ for photocatalytic HER measurements.

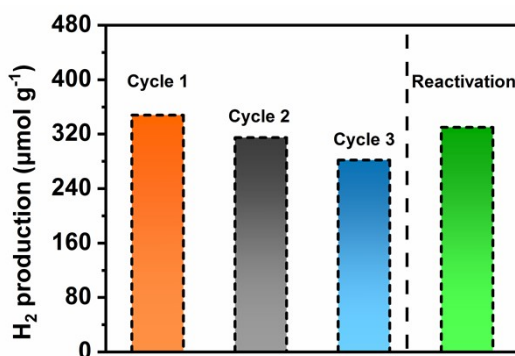


Figure S4. Reactivation measurements of photocatalytic HER performance in $\text{Chl@Cu}_2\text{O/Ti}_3\text{C}_2\text{T}_x$ samples.

Table S1. Comparison of the performance of photocatalytic hydrogen production with other similar efforts.

Composite	Sacrificial agent	Rate ($\mu\text{mol/h/g}$)	Refs.
SQ/Ti ₃ C ₂ T _x	55 mM AA	28.6	S3
Dye@Ti ₃ C ₂ T _x	55 mM AA	15.5	S4
Chl/Ti ₃ C ₂ T _x	55 mM AA	52	S5
g-C ₃ N ₄ /Ti ₃ C ₂ T _x	10 vol% TEOA	88	S6
EY/Ti ₃ C ₂ T _x	10 vol% TEOA	33.4	S7
Chl@Cu ₂ O/Ti ₃ C ₂ T _x	55 mM AA	174	This work

Table S2. The fitting data of Nyquist plots for Chl@Ti₃C₂T_x, Cu₂O/Ti₃C₂T_x and Chl@Cu₂O/Ti₃C₂T_x.

Sample	R ₁ / Ω	R ₂ / Ω	CPE-T/ 10^{-3}	CPE-P	W _{O-R}	W _{O-T}	W _{O-P}
Chl@Ti ₃ C ₂ T _x	6.7	110.3	0.75	0.61	4.9	0.15	0.28
Cu ₂ O/Ti ₃ C ₂ T _x	6.6	99.1	1.10	0.57	6.7	0.36	0.29
Chl@Cu ₂ O/Ti ₃ C ₂ T _x	6.3	60.7	1.21	0.54	5.1	0.95	0.22

References

- S1. H. Tamiaki, A.R. Holzwarth, K. Schaffner, A synthetic zinc chlorin aggregate as a model for the supramolecular antenna complexes in the chlorosomes of green bacteria, *J. Photochem. Photobiol. B: Biol.* 15 (1992) 355-360.
- S2. H. Tamiaki, M. Amakawa, Y. Shimono, R. Tanikaga, A.R. Holzwarth, K. Schaffner, Synthetic zinc and magnesium chlorin aggregates as models for supramolecular antenna complexes in chlorosomes of green photosynthetic bacteria, *Photochem. Photobiol.* 63 (1996) 92-99.
- S3 Y. Liu, Y. Li, A. Li, Y. Gao, X.-F. Wang, R. Fujii, S. Sasaki, *J. Colloid Interface Sci.* 633 (2023) 218-225.
- S4 X. Sun, Y. Li, X.-F. Wang, R. Fujii, Y. Yamano, O. Kitao, S. Sasaki, *New J. Chem.* 46 (2021) 2166-2177.
- S5 Y. Li, X. Chen, Y. Sun, X. Meng, Y. Dall'Agnese, G. Chen, C. Dall'Agnese, H. Ren, S. Sasaki, H. Tamiaki, X.-F. Wang, *Adv. Mater. Interfaces* 7 (2020) 1902080.
- S6 Y. Sun, D. Jin, Y. Sun, X. Meng, Y. Gao, Y. Dall'Agnese, G. Chen, X.-F. Wang, *J. Mater. Chem. A* 6 (2018) 9124-9131.
- S7 Y. Sun, Y. Sun, X. Meng, Y. Gao, Y. Dall'Agnese, G. Chen, C. Dall'Agnese, X.-F. Wang, *Catal. Sci. Technol.* 9 (2019) 310-315.